Organic & Biomolecular Chemistry

PAPER

View Article Online
View Journal | View Issue

Dimerization of a heat shock protein 90 inhibitor enhances inhibitory activity†

Cite this: *Org. Biomol. Chem.*, 2014, **12**, 765

Hendra Wahyudi, Yao Wang and Shelli R. McAlpine*

Received 22nd August 2013,
Accepted 5th November 2013

DOI: 10.1039/c3ob41722k

www.rsc.org/obc

Heat shock protein 90 (hsp90) accounts for 1–2% of the total proteins in normal cells and it functions as a dimer. Hsp90 behaves as a molecular chaperone that folds, assembles, and stabilizes client proteins. We have developed a novel hsp90 inhibitor, and herein we describe the synthesis and biological activity of the dimerized variant of this inhibitor. Tethering a monomer inhibitor together produced a dimerized compound that more effectively inhibits hsp90 over the monomer.

Introduction

Heat shock protein 90 (hsp90) is a ubiquitous molecular chaperone that facilitates the assembly and regulates the folding of proteins that are important in molecular signalling events.[1] In normal cells, expression of hsp90 accounts for 1–2% of cytosolic protein, whereas in cancer cells it is 3–6%.[1–7] This overexpression of hsp90 is primarily driven by high levels of cell signalling events that occur during oncogenic cell growth, which causes stress and leads to the heat shock response being induced (including hsp90). To date, there are over 100 client proteins associated with hsp90 that are involved in the molecular signalling pathways of cancer cells.[1,8–12] Hsp90 functions as a dimer and it contains three domains: N-, middle- and C-domains.[13,14] The ATP binding site (located in the N-domain) is the target for all hsp90 inhibitors in clinical trials.[15] The major drawback to these clinical candidates, including 17AAG (our positive control) is the induction of a heat shock response that occurs when the inhibitors bind to hsp90's ATP-binding domain.[16] In order to avoid the heat shock rescue response, compounds that do not target the ATP-binding site are utilized, and several examples of allosteric modulators and C-terminal inhibitors have shown that the heat shock response is not induced when modulating the C-terminus, but only when blocking the ATP binding site of the N-terminus.[17–20]

We have developed several hsp90 inhibitors, all of which bind to hsp90 between its N-middle domain, and allosterically modulate C-terminal clients and co-chaperones from binding to hsp90.[18–34] Of these inhibitors, SM122 (Fig. 2) displayed reasonable cytotoxicity (IC_{50} = 3.5 μM against pancreatic cancer cell line PL45; IC_{50} = 3.9 μM against colon cancer cell line HCT-116) and it had a unique phenotype of allosterically inhibiting access to hsp90's C-terminal domain. SM122 has already been reported to preferentially bind to hsp90's closed twisted conformation (Fig. 1); based on FP anisotropy of SM122 against Hsc82 (full-length yeast homolog of hsp90), K_d of SM122 to open state Hsc82 is 103 ± 46 μM *versus* 55 ± 21 μM in closed-stated conformation.[31] Thus, we investigated the hypothesis of whether the combination of two SM122 molecules using a polyethylene glycol (PEG) chain would enhance the inhibitory activity against hsp90 dimer.[29,34] Regulating signal transduction events of two proteins was successfully accomplished by Scheiber *et al.* utilizing dimerized molecules.[35,36] This strategy was exemplified in the synthesis of FK1012, a dimer variant of immunosuppressant FK506, where the dimer diminished the toxicity of FK506 associated with calcineurin inhibition, but retained immunosuppressant activity at considerably lower doses than FK506.[35]

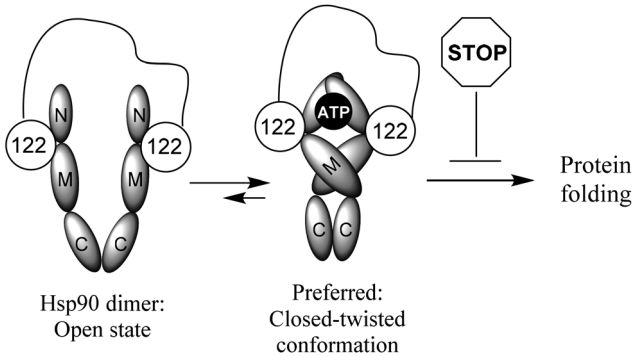

Fig. 1 Design element behind dimerizing SM122. Our goal is to trap the closed-twisted conformation of hsp90.

Department of Chemistry, University of New South Wales, Sydney, NSW 2052, Australia. E-mail: s.mcalpine@UNSW.edu.au; Fax: +61-2-9385-6111; Tel: +61-4-1672-8896

†Electronic supplementary information (ESI) available: ^{1}H-, ^{13}C-NMR spectra, LCMS, HRMS, solubility, luciferase assay and protein binding assay data for SM122-PEG conjugate and DIMERs are provided. See DOI: 10.1039/c3ob41722k

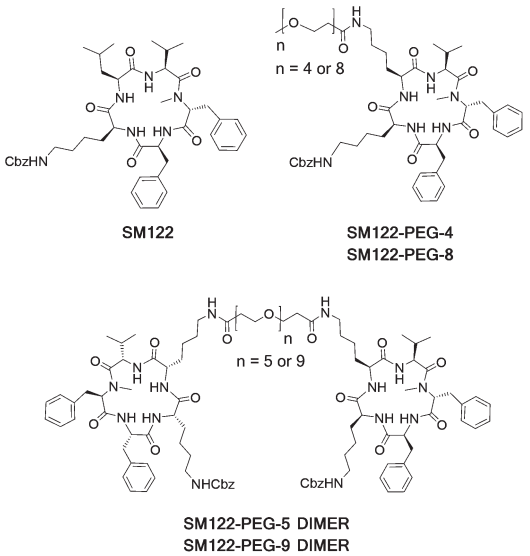

Fig. 2 Development of SM122 variants: structures of SM122, and SM122–PEG conjugate or SM122–PEG DIMER.

In 2011, dimerisation of novobiocin, an hsp90 C-terminal inhibitor, utilizing variety of linker lengths and types produced coumermycin A1 analogues that were more potent and selective than monomeric novobiocin.[37] Considering that hsp90 functions as a dimer, one strategy for enhancing SM122 as a clinical candidate is to halt hsp90 function by stabilizing the protein dimer (Fig. 1) using a dimerized molecule that preferred the closed-twisted conformation.

Herein we describe our dimerization approach for advancing our novel hsp90 inhibitor, SM122, into a more effective inhibitor over the parent compound. Dimerizing SM122 using PEG linkers (Fig. 2), we tested our compounds in hsp90 activity assays (luciferase refolding assays) in order to evaluate their activity compared to the parent SM122. We also prepared control compounds SM122–PEG-4 and SM122–PEG-8 that were monomers with PEG (Fig. 2). We observed that the inhibitory effects of DIMERs on hsp90 chaperone function are significantly greater than either the monomer or the PEG-monomer controls (~2-fold, Fig. 3a). Examining the compounds' ability to inhibit binding between hsp90 and its essential co-chaperone proteins HOP and FKBP52 showed that the inhibitory effects of SM122–PEG DIMER is 18–39% greater than SM122–PEG or SM122.

Results and discussion

Design

Previous work on SM122 had shown that replacing a leucine with a lysine and attaching the compound to a PEG-biotin moiety did not inhibit binding of SM122 to hsp90.[29,34] Thus, we chose this position to attach the PEG linker. In the synthesis of SM122–PEG conjugate, two different PEG chains (4-PEG and 8-PEG units) were chosen to examine the impact of the PEG length on the hsp90 binding and as controls for the

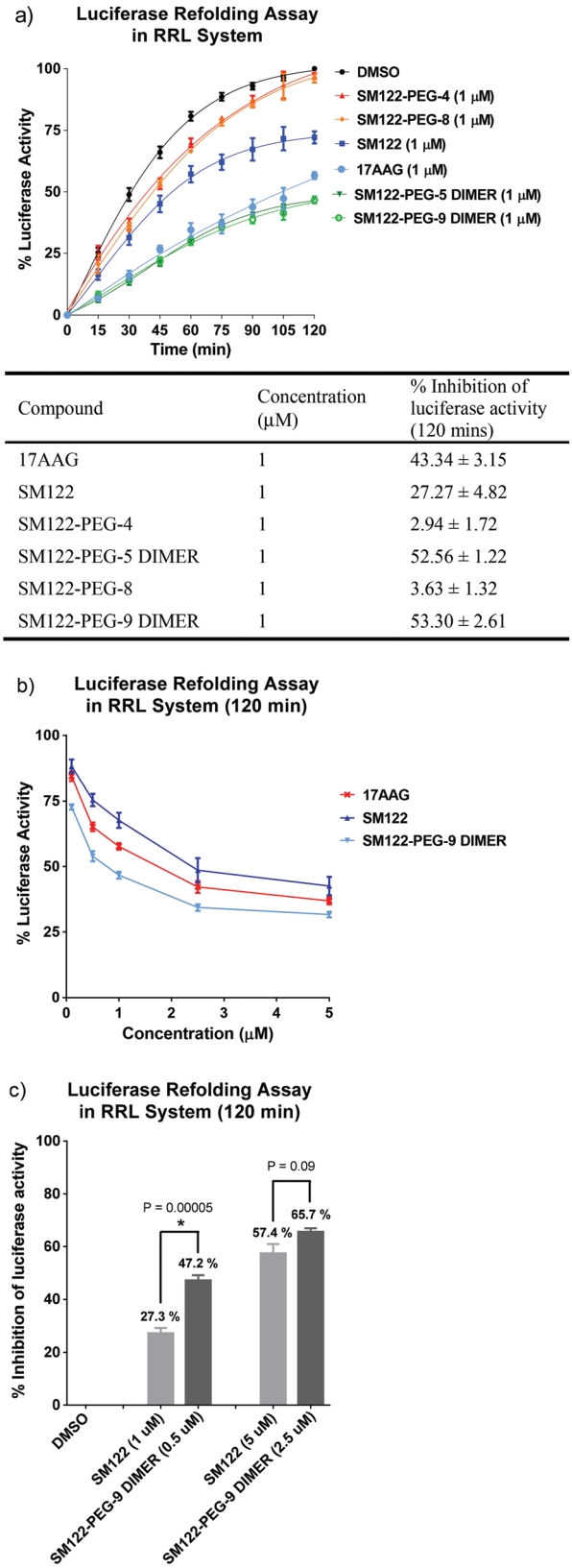

Compound	Concentration (μM)	% Inhibition of luciferase activity (120 mins)
17AAG	1	43.34 ± 3.15
SM122	1	27.27 ± 4.82
SM122-PEG-4	1	2.94 ± 1.72
SM122-PEG-5 DIMER	1	52.56 ± 1.22
SM122-PEG-8	1	3.63 ± 1.32
SM122-PEG-9 DIMER	1	53.30 ± 2.61

Fig. 3 (a–c) Luciferase refolding assay: comparison of compounds' inhibitory activity using an hsp90-mediated protein folding assay (*P-value ≤ 0.05).

dimerized SM122 compounds.[38] In the SM122–PEG DIMER synthesis, we used two different linker lengths, 5-PEG and 9-PEG units, in order (a) to correlate to the monomer-PEG analogs (4-PEG and 8-PEG) and (b) to probe the optimal linker length that would facilitate binding to hsp90.

We chose the PEG length based upon the crystal structure of full yeast hsp90-p23/Sba1 complex as reported by Pearl.[18,39–41] Lee *et al.* also showed that in an open state of hsp90, the inner distance between the Middle C-domains are 30 Å apart, and the outer distance is 70 Å apart.[42] Based on the work of Agard *et al.*[40] the open conformation of hsp90's N-middle domain is estimated to be 80 Å apart. Since the crystal structure of human hsp90 in the closed twisted conformation is currently unknown, we selected PEG lengths ~30–40 Å (5-PEG and 9-PEG units), which approximately equal to the inner distance or half of the outer distance of the N-middle domain of the two monomers of one hsp90 protein.[34,40]

Synthesis

Synthesis of **2**, a precursor for both SM122–PEG and SM122–PEG DIMER, was afforded *via* solid phase peptide synthesis (Scheme 1). Using a synthetic approach previously reported for making biotinylated tagged derivatives[29] we started with preloaded 2-chlorotrityl-phenylalanine (Phe) resin. Subsequent coupling of Fmoc-protected amino acids and amine deprotections led to a solid phase bound linear analog. Cleavage of the compound from the resin and cyclization yielded **1**. Deprotection of the lysine residue generated **2**.

Conversion of **2** into SM122–PEG was accomplished by coupling a methyl-capped PEGylated (4 or 8 PEG units) *N*-hydroxysuccinimidyl ester to **2** (1.0 equivalents of the linker, Scheme 2). Generating the dimer was accomplished in a similar manner, but utilized a PEGylated (5 or 9 PEG units) homobifunctional bis-*N*-hydroxysuccinimidyl ester to **2** (0.5 equivalents of the linker, Scheme 2).

Hsp90-dependent luciferase refolding assay

Assessing the direct inhibition of the hsp90 protein folding machinery with our compounds provides information on which analogue binds most effectively to hsp90 and inhibits its protein folding function. Utilizing an hsp90-dependent luciferase-refolding assay with rabbit reticulocyte lysate (RRL) refolding system produces a luminescent signal when hsp90 is active and functioning. Addition of hsp90 inhibitors to the RRL system shows a decrease in luminescence that is directly correlated to the compound's inhibition activity of hsp90.

Our data show that DMSO (negative control, black line, Fig. 3a) behaved similar to the PEG conjugates (SM122–PEG-4 and SM122–PEG-8, red and orange lines respectively, Fig. 3a) and the PEG motifs alone (*i.e.* no compound, see MS (PEG)s and BS (PEG)s, ESI†). Both 17-AAG and SM122 inhibited hsp90 activity (light blue and dark blue lines respectively, Fig. 3a). However, the inhibitory activity was significantly improved when using the dimers SM122–PEG-5 DIMER and SM122–PEG-9 DIMER (dark and light green respectively, Fig. 3a). Significantly, SM122–PEG-5 DIMER and SM122–PEG-9 DIMER are ~15- to 18-fold more effective than their SM122–PEG conjugates and PEG motifs respectively (Table, Fig. 3a). Our data indicate that the inhibitory activity against the hsp90-mediated

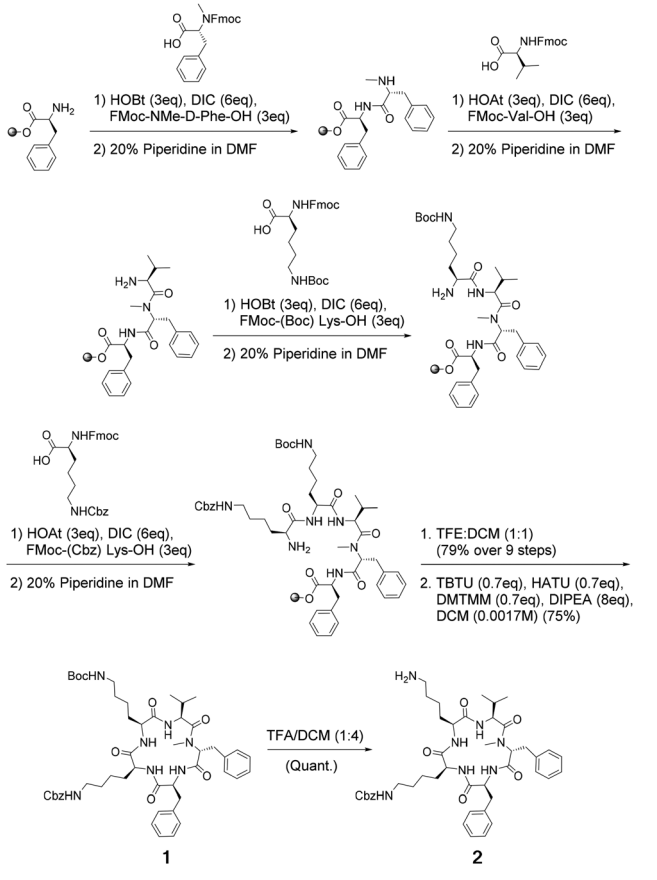

Scheme 1 Solid phase peptide synthesis of compound **2**, a precursor to SM122–PEG conjugate and SM122–PEG DIMER.

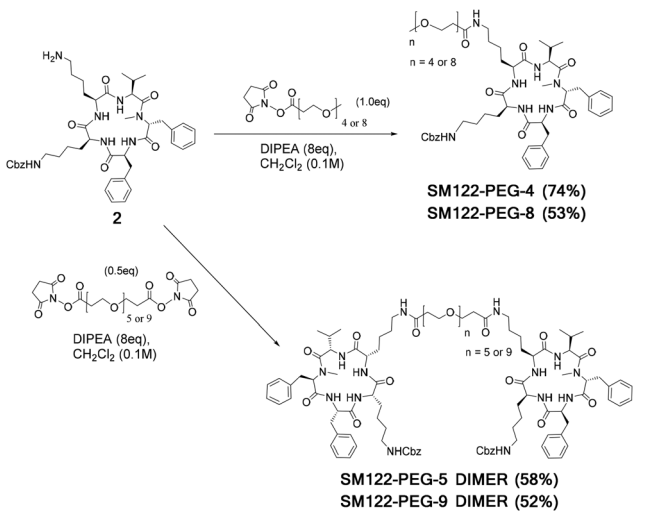

Scheme 2 Synthesis of SM122–PEG conjugates and SM122–PEG DIMERs.

refolding of denatured luciferase is due to the dimerization of SM122 rather than an increase the solubility effect of PEG. Indeed a deleterious effect is seen when adding PEG to the compound. We believe that this is due to the inherent "sticky" quality of PEG, which blocks access to the compound if not utilized for compound binding.

Running additional luciferase assays (Fig. 3b), where multiple compound concentrations were run, clearly show the same trends where even at twice the concentration of the dimer, SM122 never reaches the inhibitory ability of SM122–PEG-9. Specifically, comparing SM122 (1 μM) and SM122–PEG-9 DIMER (0.5 μM) shows that the DIMER is still significantly more active than the monomer despite the same number of SM122 molecules being present (Fig. 3c). This trend is also observed at 5 μM of SM122 and 2.5 μM of DIMER. Taken together, these results provide strong evidence that dimerization is a successful way to improve the efficiency of SM122 molecule in suppressing the chaperone function of hsp90 protein acting as a dimer.

Protein binding assay

In order to evaluate the direct impact of these compounds on hsp90, we examined their efficiency in blocking the binding interaction between hsp90 and HOP (hsp organizing protein) as well as hsp90 and FKBP52 (an immunophilin that regulates hormone receptors). It has been demonstrated that both proteins, HOP and FKBP52, bind to the C-terminus of hsp90, and SM122 blocks the interaction between hsp90 and both of these proteins.[18,43] Thus, this is an ideal assay to compare the effectiveness of SM122–PEG DIMER and SM122. Protein binding assays showed that 10 μM of SM122–PEG-9 DIMER was 1.3-fold more effective in inhibiting binding between hsp90 and HOP than 20 μM of SM122 (P-value = 0.002, Fig. 4a), indicating that the DIMER is more efficient at interfering with the hsp90–HOP interaction than SM122 monomer alone. Additional evidence supports these conclusions, where 10 μM of SM122–PEG-9 DIMER blocked the binding between hsp90-FKBP52 by 1.4-fold greater than 20 μM of SM122 alone (Fig. 4b).

Interestingly, both the 20 and 10 μM SM122 have the same effect at blocking the binding between hsp90 and HOP, which suggests that the monomer compound has maximized its binding. This could be related to the solubility, however, as discussed in the next section, because PEG dramatically increases their solubility, addition of PEG to the monomer should dramatically improve SM122's ability to block binding. As is observed in both Fig. 4a and 4b, addition of PEG does not enhance the activity of SM122 for either protein with hsp90 (compare SM122 activity *versus* SM122–PEG-8).

Solubility determination

Since the PEG linker is known to increase solubility of drug molecules, one hypothesis is that the increase in solubility of the DIMER is responsible for the observed improvement of activity. Thus, the solubility of SM122–PEG conjugates and DIMERs were determined. The method for solubility evaluation is annotated in the ESI.† The results (summarized in Table 1 below) show that SM122–PEG-8, the least active hsp90 inhibitor, was the most soluble compound, identified as ~200-fold more soluble than SM122. In contrast, the DIMERs (SM122–PEG-5 DIMER and SM122–PEG-9 DIMER) were only ~4- and ~6-fold respectively more soluble than SM122. The PEG monomer compounds (SM122–PEG-4 and PEG-8 respectively) were completely ineffective in the luciferase assay. These indicate that solubilizing the compound is not enough to produce activity. Given that the RRL luciferase assay is run with large quantities of cytosol, it is likely that the sticky PEG

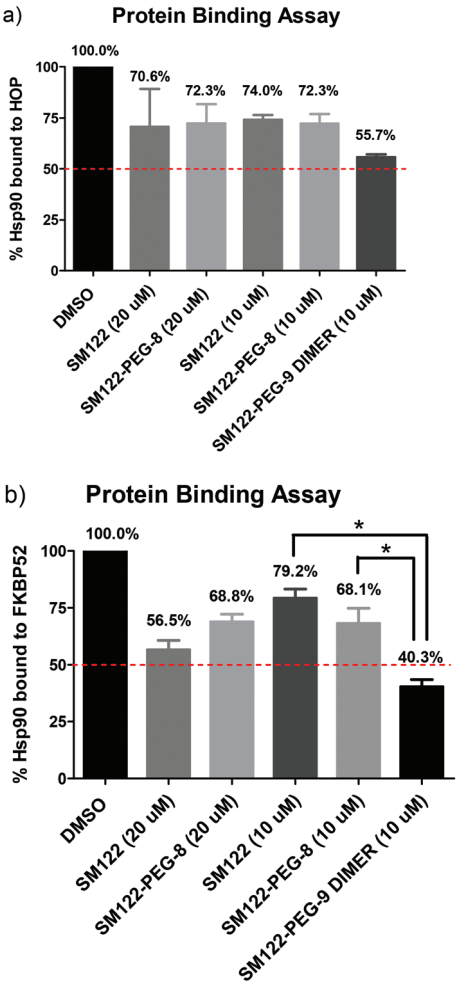

Fig. 4 The inhibitory effects of SM122, SM122–PEG-8 and SM122–PEG-9 DIMER on the binding between hsp90 and its co-chaperone (a) HOP and (b) FKBP52 (*P-value ≤ 0.05).

Table 1 Solubility of SM122, SM122–PEG conjugates, and SM122–PEG DIMERs

Compound	(μg mL^{-1})	(μM)
SM122	0.66 ± 0.28	0.84 ± 0.35
SM122–PEG-4	6.45 ± 0.36	6.36 ± 0.35
SM122–PEG-5 DIMER	7.00 ± 0.71	3.69 ± 0.37
SM122–PEG-8	198.64 ± 3.89	166.69 ± 3.27
SM122–PEG-9 DIMER	10.18 ± 1.72	4.91 ± 0.83

linkers block the ability of SM122 to find hsp90 and inhibit its function.

In contrast, biochemical assays, which did not have sticky cytosolic proteins in the assays, showed that the SM122–PEG-8 analog was as effective at inhibiting the binding between HOP and hsp90 (Fig. 4a). These data support the conclusion that solubility plays little role in the effectiveness of the compounds. Interestingly, the effect of PEG does appear to be deleterious when comparing the binding of 20 μM SM122 to SM122–PEG-8 but not when comparing the activity of 10 μM of each molecule. In both cases, however, the data indicate that solubility plays little- to no-role in the biological activity of the molecules. Finally, the DIMER, although not as soluble as the PEG monomer, is significantly more active in both binding assays.

Dimer binding mode

The data observed from luciferase refolding assay and protein binding assay also revealed the possible interactions that occurred when SM122–PEG DIMER bound to hsp90. Based on the cooperative binding theory, when one SM122 unit binds to the hsp90 dimer it may induce an allosteric modulation across one side of the dimer protein, resulting in a conformational shift that allows a second SM122 molecule to bind to the other side of the hsp90 dimer with lower binding energy than monomer alone. Alternatively, the binding event of SM122 can compromise the secondary binding event. In our case, inducing a positive binding event and lowering the energy for a second SM122 molecule to bind explains the data observed in Fig. 3b. Specifically, SM122 (1 μM) and SM122–PEG-9 DIMER (0.5 μM) and SM122 (5 μM) and SM122–PEG-9 DIMER (2.5 μM) both show that the DIMER is still significantly more active than the monomer despite the same number of SM122 molecules being present (Fig. 3c). Thus, the dimer is more effective than two equivalents of the monomer (Model B, Fig. 5).

An alternative theory is that Model A (Fig. 5) may exist. However, since the DIMER showed higher inhibitory efficacy than the monomer at the same concentration levels (Fig. 3c), a single SM122–PEG DIMER must bind to more than one hsp90 dimer protein. However our data shows that the two "monomers" of the SM122–PEG dimer are *not* acting independently (Fig. 5, Model A). That is, the two SM122 molecules in the PEG dimer are not acting as two separate SM122 molecules. If they had been behaving independently, we would see that the dimer would be twice as effective at the same concentration and at half the concentration the dimer would be as effective as the monomer. As discussed above this is not the case, in all assays, the dimer is more effective than the monomer regardless of concentration, which is indicative of a synergistic binding event of both SM122 molecules tethered together (Model B, Fig. 5).

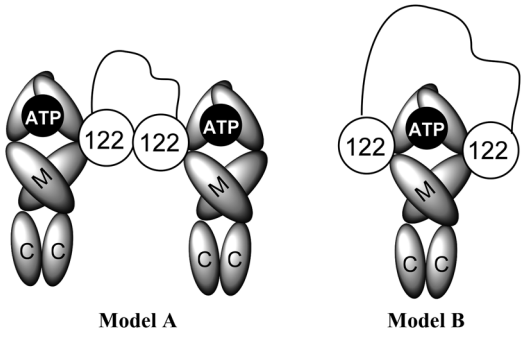

Fig. 5 Dimer binding mode: Model A *versus* Model B.

In summary, we have shown that dimerizing SM122, a novel hsp90 inhibitor, will effectively modulate hsp90's activity. Furthermore, we have shown that dimerization of SM122 produces a synergistic inhibitor, that more effectively inhibits hsp90 activity from refolding proteins, and blocks binding between client and co-chaperone proteins and hsp90 than monomer alone. We also show that the DIMER effectiveness is not related to its improved solubility, and that the DIMER is most effective when bound to the same hsp90 dimer *versus* two separate hsp90 dimers. These studies demonstrate that dimerizing an hsp90 inhibitor is more effective at blocking hsp90 activity than using monomer alone.

Experimental

General information

All reactions were carried out under N_2 atmosphere with dry solvent under anhydrous conditions, unless indicated otherwise. Reagents were commercially obtained without further purification, unless otherwise stated. Reaction was monitored *via* thin-layer chromatography (TLC) carried out on silica gel plates using UV light at λ = 254 nm for visualization, and potassium permanganate in water with heat and developing agents. Silica gel was used for flash chromatography. NMR spectra were obtained at 298 K. LC/MS was recorded on an LCMS system connected to a trap running in positive electrospray ionization (ESI+) mode. The mobile phase was composed of DDI water with 0.1% (v/v) formic acid (solvent A), and HPLC grade acetonitrile with 0.1% (v/v) formic acid (solvent B). The gradient elution was conducted as follows: flow rate 0.5 mL min^{-1}; initial 70% solvent A, 30% solvent B; at 4 minutes 100% solvent B; at 12 minutes 70% solvent A, 30% solvent B. Semipreparative reversed-phase HPLC was carried out on an LCMS system. The mobile phase was composed of DDI water with 0.1% (v/v) formic acid (solvent A), and HPLC grade acetonitrile with 0.1% (v/v) formic acid (solvent B). The gradient elution was conducted as follows: flow rate 2 mL min^{-1}; initial 70% solvent A, 30% solvent B hold for 35 minutes; at 35 minutes 100% solvent B hold for 13 minutes; at 48 minutes 70% solvent A, 30% solvent B hold for 2 minutes.

General solid phase synthesis remarks

Stepwise solid phase peptide synthesis was performed in a polypropylene solid-phase extraction cartridge fitted with a 20 μm polyethylene frit purchased from Applied Separations

(Allentown, PA). 2-Chlorotrityl resins were purchased in pre-loaded form with L-Phe. Resins were swelled in dimethylformamide (DMF) for 30 minutes prior to assembly of the linear five-residue peptide sequence. Solid-phase syntheses were performed on a 0.5 mmol scale based on resin-loading. All operations were performed at room temperature under open atmosphere unless stated otherwise.

General solid phase peptide synthesis

Fmoc-protected amino acids were coupled using 3.0 equiv. of amino acid, 3.0 equiv. of 1-hydroxybenzotriazole (HOBt), and 6.0 equiv. of diisopropylcarbodiimide (DIC). Couplings were performed in DMF at 0.2 M with respect to the incoming Fmoc-protected amino acid. Couplings were allowed to proceed for a minimum of 2 hours, and were assayed *via* ninhydrin test to verify completion. Once complete, the coupling reaction solution was drained, and the resin subjected to Fmoc deprotection. (Note: Fmoc and *N*-methyl amino acids are coupled according to the cycle above, however for subsequent coupling onto the secondary amino terminus, 1-hydroxybenzotriazole was substituted with 1-hydroxy-7-azabenzotriazole (HOAt) and the coupling was allowed to proceed overnight.)

General solid phase amine deprotection

Following coupling completion, the peptide-resin was treated as follows for removal of the Fmoc protecting group: DMF wash (3 × 1 minute), 20% piperidine–DMF (1 × 5 minutes), 20% piperidine–DMF (1 × 10 minutes), DMF wash (2 × 1 minute), IPA wash (1 × 1 minute), DMF wash (1 × 1 minute), IPA (1 × 1 minute), DMF (3 × 1 minute). A ninhydrin test was performed to verify completion.

General N-terminal solid phase amine deprotection

Once the final N-terminal amino acid residue had been coupled, the peptide-resin was treated as follows for removal of the Fmoc protecting group: DMF wash (3 × 1 minute), 20% piperidine–DMF (1 × 5 minutes), 20% piperidine–DMF (1 × 10 minutes), DMF wash (3 × 1 minute), IPA wash (3 × 1 minute), MeOH (3 × 1 minute). The fully-assembled peptide-resin was then drained and dried *in vacuo* overnight.

Cleavage of linear peptide

The full-length, linear peptide was cleaved from the resin by swelling and shaking the peptide-resin for 24 hours in a 1 : 1 (v/v) 2,2,2-trifluoroethanol (TFE)–CH_2Cl_2 (10 volumes per gram of dried resin). The cleavage solution was filtered through a Buchner filter, and the drained resin was washed with additional CH_2Cl_2 (5 volumes per gram of initial dried peptide-resin) to fully extract the cleaved peptide from the resin. Solvents in the combined filtrates were evaporated by rotary evaporation and the solids dried *in vacuo* overnight. The solids were then reconstituted in CH_2Cl_2, evaporated by rotary evaporation and dried *in vacuo* overnight again to remove residual entrapped TFE.

Macrocyclization procedure (syringe pump)

Three coupling agents (DMTMM, HATU, and TBTU) were used at 0.8 equiv. each. These coupling agents were dissolved in 4/5 of a calculated volume of dry CH_2Cl_2 that would give a 0.001 M overall concentration when included in the volume used for the deprotected peptide. The crude, dry, double deprotected peptide (free acid and free amine) was dissolved in the other 1/5 solvent volume of CH_2Cl_2. DIPEA (8.0 equiv.) was then added to the solution containing coupling reagents dissolved in CH_2Cl_2. The double deprotected peptide was then added to the bulk solution dropwise using a syringe pump at a rate of 30 mL h^{-1}. The reaction was monitored *via* LCMS and generally complete in 1–2 hours. Upon completion, the reaction was worked up by washing with aqueous HCl (pH 1) and saturated sodium bicarbonate. After back extraction of aqueous layers with large quantities of CH_2Cl_2, the organic layers were combined, dried, filtered and concentrated. All macrocycles were first purified by flash column chromatography using an ethyl acetate–hexane gradient on silica gel. Finally, when necessary, reversed-phase HPLC was used for additional purification using a gradient of acetonitrile and deionized water with 0.1% TFA.

Synthesis

Macrocycle Phe-D-N-Me-Phe-Val-Leu-Lys (Cbz) (SM122). Synthesis of Macrocycle Phe-D-N-Me-Phe-Val-Leu-Lys (Cbz) was referenced from the published data (Sellers, R. P., Alexander, L. D., Johnson, V. A., Lin, C.-C., Savage, J., Corral, R., Moss, J., Slugocki, T. S., Singh, E. K., Davis, M. R., *et al.* A third generation of Sansalvamide A derivatives: Design and synthesis of Hsp90 Inhibitors. *Bioorg. Med. Chem.*, 2010, **18**, 6822–6856; compound 28).

Macrocycle Phe-N-Me-D-Phe-Val-Lys (Boc)-Lys (Cbz) (compound 1). Synthesis of Macrocycle Phe-D-N-Me-Phe-Val-Lys (Boc)-Lys (Cbz) was referenced from the published data (Kunicki, J. B., Petersen, M. N., Alexander, L. D., Ardi, V. C., McConnell, J. R., and McAlpine, S. R. Synthesis and Evaluation of Biotinylated Sansalvamide A Analogs and their Modulation of Hsp90. *Bioorg. Med. Chem. Lett.*, 2011, **21**, 4716–4719; compound **2**-T-IV).

Macrocycle Phe-N-Me-D-Phe-Val-Lys-Lys (Cbz) (compound 2)

Macrocycle Phe-N-Me-D-Phe-Val-Lys-Lys (Cbz) was synthesized by removing the Boc from macrocycle Phe-N-Me-D-Phe-Val-Lys (Boc)-Lys (Cbz). Utilizing 206 mg (0.23 mmol, 1.0 equiv.) of Phe-N-Me-D-Phe-Val-Lys (Boc)-Lys (Cbz), 0.46 mL of trifluoroacetic acid, 1.84 mL of CH_2Cl_2 (183.5 mg, Quant. yield).

Compound SM122–PEG-5 DIMER

Utilizing 102 mg (0.13 mmol, 1.0 equiv.) of Phe-N-Me-D-Phe-Val-Lys-Lys (Cbz), 68.0 μL (64 μmol, 0.5 equiv.) BS(PEG)5, and 0.18 mL (8.0 equiv.) of DIPEA dissolved in 13.0 mL CH_2Cl_2, under N_2. The reaction was monitored *via* LCMS and generally complete in 1–2 hours. Upon completion, the reaction was worked up by washing with aqueous HCl (pH 1) and saturated

sodium bicarbonate. After back extraction of aqueous layers with large quantities of CH_2Cl_2, the organic layers were combined, dried, filtered and concentrated. The crude material was purified using column chromatography (silica gel, EtOAc–MeOH) to yield 70 mg (58% yield) of the compound. R_f: 0.39 (EtOAc–MeOH 9 : 1); δH NMR (300 MHz, $CDCl_3$): δ 0.80–0.85 (d, J = 6.71 Hz, 6H, $CHCH(CH_3)_2$); 0.88–0.94 (d, J = 6.71 Hz, 6H, $CHCH(CH_3)_2$); 0.95–1.08 (m, 4H, $CH_2\gamma$ Lys (PEG)); 1.27–1.30 (m, 4H, $CH_2\delta$ Lys (Cbz)); 1.34–1.46 (m, 4H, $CH_2\gamma$ Lys (Cbz)); 1.48–1.58 (m, 4H, $CH_2\delta$ Lys (PEG)); 1.69–1.82 (m, 4H, $CH_2\beta$ Lys (PEG)); 1.92–2.03 (m, 4H, $CH_2\beta$ Lys (Cbz)); 2.14–2.23 (m, 4H, $CH_2\beta$ Val); 2.47–2.50 (t, 4H, $COCH_2$ (PEG)); 2.83–2.88 & 3.05–3.14 (m, 4H, $CH_2\beta$ Phe); 2.85–2.92 (s, 6H, NMe); 2.96–3.02 & 3.14–3.24 (m, 4H, $CH_2\beta$ D-Phe); 3.04–3.20 (m, 4H, $CH_2\varepsilon$ Lys (PEG)); 3.15–3.30 (m, 4H, $CH_2\varepsilon$ Lys (Cbz)); 3.54–3.60 (m, 4H, CH_2 (PEG)); 3.61–3.78 (m, 12H, CH_2 (PEG)); 3.75–3.83 (m, 2H, CHα Lys (PEG)); 3.93–4.01 (m, 2H, CHα Lys (Cbz)); 4.44–4.52 (m, 2H, CHα Val); 4.72–4.82 (m, 2H, CHα Phe); 5.07–5.13 (s, 4H, CH_2 Cbz); 5.16–5.23 (m, 2H, CHα D-Phe); 5.49–5.57 (m, 2H, NH); 6.80–6.87 (m, 2H, NH); 6.87–6.95 (m, 2H, NH); 7.01–7.37 (m, 30H, Ph); 7.65–7.72 (m, 2H, NH). δC NMR (75 MHz, $CDCl_3$): δ 18.0, 19.6, 22.7, 23.4, 28.9, 29.2, 29.6, 30.3, 30.5, 30.7, 32.9, 36.8, 37.8, 38.2, 40.8, 54.0, 54.9, 55.3, 57.1, 57.3, 59.0, 66.5, 67.3, 70.5, 71.8, 126.9, 127.9, 128.0, 128.5, 128.6, 128.7, 128.8, 129.4, 136.1, 136.5, 136.8, 156.7, 169.7, 171.7, 172.1, 172.7; LC/MS (ESI): m/z called for $C_{102}H_{140}N_{14}O_{21}$ (M + H^+) = 1897.03, found 950.00 (half-mass); HRMS (ESI-TOF): M + Na^+ + H^+ found 1921.0233 $C_{102}H_{141}N_{14}O_{21}Na$ requires 1921.0293.

Compound SM122–PEG-9 DIMER. Utilizing 180 mg (0.23 mmol, 1.0 equiv.) of Phe-N-Me-D-Phe-Val-Lys-Lys (Cbz), 161.0 μL (113 μmol, 0.5 equiv.) BS (PEG)9, and 0.31 mL (8.0 equiv.) of DIPEA dissolved in 20.0 mL CH_2Cl_2, under N_2. The reaction was monitored *via* LCMS and generally complete in 1–2 hours. Upon completion, the reaction was worked up by washing with aqueous HCl (pH 1) and saturated sodium bicarbonate. After back extraction of aqueous layers with large quantities of CH_2Cl_2, the organic layers were combined, dried, filtered and concentrated. The crude material was purified using column chromatography (silica gel, EtOAc–MeOH) to yield 123 mg (52% yield) of the compound. R_f: 0.56 (EtOAc–MeOH 6 : 4); δH NMR (300 MHz, $CDCl_3$): δ 0.80–0.85 (d, J = 6.71 Hz, 6H, $CHCH(CH_3)_2$); 0.88–0.94 (d, J = 6.71 Hz, 6H, $CHCH(CH_3)_2$); 0.95–1.08 (m, 4H, $CH_2\gamma$ Lys (PEG)); 1.27–1.30 (m, 4H, $CH_2\delta$ Lys (Cbz)); 1.34–1.46 (m, 4H, $CH_2\gamma$ Lys (Cbz)); 1.48–1.58 (m, 4H, $CH_2\delta$ Lys (PEG)); 1.69–1.82 (m, 4H, $CH_2\beta$ Lys (PEG)); 1.92–2.03 (m, 4H, $CH_2\beta$ Lys (Cbz)); 2.14–2.23 (m, 4H, $CH_2\beta$ Val); 2.47–2.50 (t, 4H, $COCH_2$ (PEG)); 2.83–2.88 & 3.05–3.14 (m, 4H, $CH_2\beta$ Phe); 2.85–2.92 (s, 6H, NMe); 2.96–3.02 & 3.14–3.24 (m, 4H, $CH_2\beta$ D-Phe); 3.04–3.20 (m, 4H, $CH_2\varepsilon$ Lys (PEG)); 3.15–3.30 (m, 4H, $CH_2\varepsilon$ Lys (Cbz)); 3.54–3.60 (m, 4H, CH_2 (PEG)); 3.61–3.78 (m, 28H, CH_2 (PEG)); 3.75–3.83 (m, 2H, CHα Lys (PEG)); 3.93–4.01 (m, 2H, CHα Lys (Cbz)); 4.44–4.52 (m, 2H, CHα Val); 4.72–4.82 (m, 2H, CHα Phe); 5.07–5.13 (s, 4H, CH_2 Cbz); 5.16–5.23 (m, 2H, CHα D-Phe); 5.49–5.57 (m, 2H, NH); 6.80–6.87 (m, 2H, NH); 6.87–6.95 (m, 2H, NH); 7.01–7.37 (m, 30H, Ph); 7.65–7.72 (m, 2H, NH). δC NMR (75 MHz, $CDCl_3$): δ 18.0, 19.6, 22.7, 23.4, 28.9, 29.2, 29.6, 30.3, 30.5, 30.7, 32.9, 36.8, 37.8, 38.2, 40.8, 54.0, 54.9, 55.3, 57.1, 57.3, 59.0, 66.5, 67.3, 70.5, 71.8, 126.9, 127.9, 128.0, 128.5, 128.6, 128.7, 128.8, 129.4, 136.1, 136.5, 136.8, 156.7, 169.7, 171.7, 172.1, 172.7; LC/MS (ESI): m/z called for $C_{110}H_{156}N_{14}O_{25}$ (M + H^+) = 2073.14, found 1038.00 (half-mass); HRMS (ESI-TOF): M + Na^+ + H^+ found 2097.1290 $C_{110}H_{157}N_{14}O_{25}Na$ requires 2097.1342.

Compound SM122–PEG-4. Utilizing 124 mg (0.16 mmol, 1.0 equiv.) of Phe-N-Me-D-Phe-Val-Lys-Lys (Cbz), 155.0 μL (155 μmol, 1.0 equiv.) MS (PEG)4, and 0.22 mL (8.0 equiv.) of DIPEA dissolved in 20.0 mL CH_2Cl_2, under N_2. The reaction was monitored *via* LCMS and generally complete in 1–2 hours. Upon completion, the reaction was worked up by washing with aqueous HCl (pH 1) and saturated sodium bicarbonate. After back extraction of aqueous layers with large quantities of CH_2Cl_2, the organic layers were combined, dried, filtered and concentrated. The crude material was purified using column chromatography (silica gel, EtOAc–MeOH) to yield 116 mg (73.5% yield) of the compound. R_f: 0.35 (EtOAc–MeOH 19 : 1). δH NMR (300 MHz, $CDCl_3$): δ 0.80–0.85 (d, J = 6.71 Hz, 3H, $CHCH(CH_3)_2$); 0.88–0.94 (d, J = 6.71 Hz, 3H, $CHCH(CH_3)_2$); 0.95–1.08 (m, 2H, $CH_2\gamma$ Lys (PEG)); 1.27–1.30 (m, 2H, $CH_2\delta$ Lys (Cbz)); 1.34–1.46 (m, 2H, $CH_2\gamma$ Lys (Cbz)); 1.48–1.58 (m, 2H, $CH_2\delta$ Lys (PEG)); 1.69–1.82 (m, 2H, $CH_2\beta$ Lys (PEG)); 1.92–2.03 (m, 2H, $CH_2\beta$ Lys (Cbz)); 2.14–2.23 (m, 2H, $CH_2\beta$ Val); 2.47–2.50 (t, 2H, $COCH_2$ (PEG)); 2.83–2.88 & 3.05–3.14 (m, 2H, $CH_2\beta$ Phe); 2.85–2.92 (s, 3H, NMe); 2.96–3.02 & 3.14–3.24 (m, 2H, $CH_2\beta$ D-Phe); 3.04–3.20 (m, 2H, $CH_2\varepsilon$ Lys (PEG)); 3.15–3.30 (m, 2H, $CH_2\varepsilon$ Lys (Cbz)); 3.36–3.42 (s, 3H, OCH_3 (PEG)); 3.54–3.60 (m, 2H, CH_2 (PEG)); 3.61–3.78 (m, 10H, CH_2 (PEG)); 3.67–3.75 (m, 2H, CH_2 (PEG)); 3.75–3.83 (m, 1H, CHα Lys (PEG)); 3.93–4.01 (m, 1H, CHα Lys (Cbz)); 4.44–4.52 (m, 1H, CHα Val); 4.72–4.82 (m, 1H, CHα Phe); 5.07–5.13 (s, 2H, CH_2 Cbz); 5.16–5.23 (m, 1H, CHα D-Phe); 5.49–5.57 (m, 1H, NH); 6.80–6.87 (m, 1H, NH); 6.87–6.95 (m, 1H, NH); 7.01–7.37 (m, 15H, Ph); 7.65–7.72 (m, 1H, NH). δC NMR (75 MHz, $CDCl_3$): δ 18.0, 19.6, 22.7, 23.4, 28.9, 29.2, 29.6, 30.3, 30.5, 30.7, 32.9, 36.8, 37.8, 38.2, 40.8, 54.0, 54.9, 55.3, 57.1, 57.3, 59.0, 66.5, 67.3, 70.5, 71.8, 126.9, 127.9, 128.0, 128.5, 128.6, 128.7, 128.8, 129.4, 136.1, 136.5, 136.8, 156.7, 169.7, 171.7, 172.1, 172.7; LC/MS (ESI): m/z called for $C_{54}H_{77}N_7O_{12}$ (M + H^+) = 1015.56, found 1016.00.

HRMS (ESI-TOF): M + Na^+, found 1038.5504 $C_{54}H_{77}N_7O_{12}Na$ requires 1038.5528.

Compound SM122–PEG-8. Utilizing 124 mg (0.16 mmol, 1.0 equiv.) of Phe-N-Me-D-Phe-Val-Lys-Lys (Cbz), 68.0 μL (155 μmol, 1.0 equiv.) MS (PEG)8, and 0.22 mL (8.0 equiv.) of DIPEA dissolved in 20.0 mL CH_2Cl_2, under N_2. The reaction was monitored *via* LCMS and generally complete in 1–2 hours. Upon completion, the reaction was worked up by washing with aqueous HCl (pH 1) and saturated sodium bicarbonate. After back extraction of aqueous layers with large quantities of CH_2Cl_2, the organic layers were combined, dried, filtered and concentrated. The crude material was purified using column

chromatography (silica gel, EtOAc–MeOH) to yield 97 mg (52.5% yield) of the compound. R_f: 0.26 (EtOAc–MeOH 19 : 1); δH NMR (300 MHz, $CDCl_3$): δ 0.80–0.85 (d, J = 6.71 Hz, 3H, $CHCH(CH_3)_2$); 0.88–0.94 (d, J = 6.71 Hz, 3H, $CHCH(CH_3)_2$); 0.95–1.08 (m, 2H, $CH_2\gamma$ Lys (PEG)); 1.27–1.30 (m, 2H, $CH_2\delta$ Lys (Cbz)); 1.34–1.46 (m, 2H, $CH_2\gamma$ Lys (Cbz)); 1.48–1.58 (m, 2H, $CH_2\delta$ Lys (PEG)); 1.69–1.82 (m, 2H, $CH_2\beta$ Lys (PEG)); 1.92–2.03 (m, 2H, $CH_2\beta$ Lys (Cbz)); 2.14–2.23 (m, 2H, $CH_2\beta$ Val); 2.47–2.50 (t, 2H, $COCH_2$ (PEG)); 2.83–2.88 & 3.05–3.14 (m, 2H, $CH_2\beta$ Phe); 2.85–2.92 (s, 3H, NMe); 2.96–3.02 & 3.14–3.24 (m, 2H, $CH_2\beta$ D-Phe); 3.04–3.20 (m, 2H, $CH_2\varepsilon$ Lys (PEG)); 3.15–3.30 (m, 2H, $CH_2\varepsilon$ Lys (Cbz)); 3.36–3.42 (s, 3H, OCH_3 (PEG)); 3.54–3.60 (m, 2H, CH_2 (PEG)); 3.61–3.78 (m, 26H, CH_2 (PEG)); 3.67–3.75 (m, 2H, CH_2 (PEG)); 3.75–3.83 (m, 1H, CHα Lys (PEG)); 3.93–4.01 (m, 1H, CHα Lys (Cbz)); 4.44–4.52 (m, 1H, CHα Val); 4.72–4.82 (m, 1H, CHα Phe); 5.07–5.13 (s, 2H, CH_2 Cbz); 5.16–5.23 (m, 1H, CHα D-Phe); 5.49–5.57 (m, 1H, NH); 6.80–6.87 (m, 1H, NH); 6.87–6.95 (m, 1H, NH); 7.01–7.37 (m, 15H, Ph); 7.65–7.72 (m, 1H, NH). δC NMR (75 MHz, $CDCl_3$): δ 18.0, 19.6, 22.7, 23.4, 28.9, 29.2, 29.6, 30.3, 30.5, 30.7, 32.9, 36.8, 37.8, 38.2, 40.8, 54.0, 54.9, 55.3, 57.1, 57.3, 59.0, 66.5, 67.3, 70.5, 71.8, 126.9, 127.9, 128.0, 128.5, 128.6, 128.7, 128.8, 129.4, 136.5, 136.8, 156.7, 169.7, 171.7, 172.1, 172.7; LC/MS (ESI): m/z called for $C_{62}H_{93}N_7O_{16}$ ($M + H^+$) = 1191.67, found 1192.00; HRMS (ESI-TOF): $M + Na^+$, found 1214.6552 $C_{62}H_{93}N_7O_{16}Na$ requires 1214.6577.

Biological methods

Luciferase refolding assay. Firefly luciferase (12.5 mg mL^{-1}; Novus Biologicals) was diluted to a concentration of 2 mg mL^{-1} in stability buffer (25 mM Tricine, pH 7.8, 10 mM $MgCl_2$, 1 mM dithiothreitol, 0.1 mM EDTA, 10% (v/v) glycerol, and 10 mg mL^{-1} bovine serum albumin), and was heat denatured at 41 °C for 30 minutes. The denatured protein was further diluted (1 : 20, v/v) in stability buffer to form 0.1 mg mL^{-1} stock solution and placed on ice before refolding. 0.5 μL of compound or DMSO (Sigma-Aldrich) as a control was incubated with 48.5 μL of 50% diluted rabbit reticulocyte lysate (RRL; Promega) in Mili-Q water at 30 °C for 5 hours. Refolding was initiated by adding 1.0 μL of the denatured luciferase stock into the RRL refolding system, treated either with compounds or DMSO in advance. Reactions were performed at 30 °C. At the indicated time points (15, 30, 45, 60, 75, 90, 105 and 120 minutes), 5 μL of each reaction mixture was removed and added to 45 μL of Bright-Glo™ luciferase assay buffer (Promega) mixed with Bright-Glo™ luciferase assay substrate (Promega), which was preloaded in a white, flat-bottomed, 96 well plate (Greiner Bio-One). After incubating for 2 minutes at room temperature, the luminescence was measured using a luminometer (Berthold Orion Microplate Luminometer). Luciferase activity in refolding reactions at each time point was calculated by the formula:

$$\text{Luciferase activity } (\%) = (\text{LI}_{\text{sample}}/\text{LI}_{\text{DMSO at 120 min}}) \times 100$$

where LI indicates the luminescence intensity in each reaction. The luciferase activity in the refolding reaction with DMSO (control) at 120 minutes was considered as 100% refolding. Reported values were averaged from three independent experiments. Error bars indicate the standard deviation. Statistical analysis was performed using GraphPad Prism software.

Protein binding assay. The inhibitory effects of SM122, SM122–PEG-8 and SM122–PEG-9 DIMER on the binding between hsp90 and its co-chaperone (HOP, StressMarq Biosciences; FKBP52, Abcam) were determined using protein binding assay. 200 nM (final concentration) of human native protein hsp90 (Life Technologies) was incubated with 10 μM of compound or DMSO (Sigma-Aldrich, final concentration of DMSO was 1%) in binding buffer (20 mM tris-HCl, 150 mM NaCl, 1% Triton-X-100, pH 7.4) for 1 hour at room temperature (RT). After incubation 100 nM (final concentration) of Histidine tagged recombinant co-chaperone was added and incubated for another 1 hour at RT. The recombinant protein was fished out with Talon-Metal Affinity Resin (Clontech Laboratories) followed by three washes of the beads in binding buffer and finally boiling the beads with 5 × Laemmli sample buffer. Samples were analyzed using 4–20% Tri-Glycine gels (Life Technologies), followed by standard Western blot to detect hsp90 and its co-chaperone. The respective ratio of hsp90 to co-chaperone was analyzed *via* Image J and transformed to a percent of hsp90 bound to co-chaperone. Reported values were averaged from three independent experiments. Error bars indicate the standard deviation. Statistical analysis was performed using GraphPad Prism software.

Acknowledgements

We thank the University of New South Wales for a scholarship to H.W. and a tuition fee waiver to Y.W. We thank NHMRC (1043561) for support of Y.W.

Notes and references

1 L. Neckers, *Trends Mol. Med.*, 2002, **8**, S55–S61.
2 G. Chiosis, H. Huezo, N. Rosen, E. Mimnaugh, L. Whitesell and L. Neckers, *Mol. Cancer Ther.*, 2003, **2**, 123–129.
3 M. G. Hollingshead, M. Alley, A. M. Burger, S. Borgel, C. Pacula-Cox, H.-H. Fiebig and E. A. Sausville, *Cancer Chemother. Pharmacol.*, 2005, **56**, 115–125.
4 M. Senju, N. Sueoka, A. Sato, K. Iwanaga, Y. Sakao, S. Tomimitsu, M. Tominaga, K. Irie, S. Hayashi and E. Sueoka, *J. Cancer Res. Clin. Oncol.*, 2006, **132**, 150–158.
5 Y.-S. Chang, L.-C. Lee, F.-C. Sun, C.-C. Chao, H.-W. Fu and Y.-K. Lai, *J. Cell. Biochem.*, 2006, **97**, 156–165.
6 D. Matei, M. Satpathy, L. Cao, Y.-C. Lai, H. Nakshatri and D. B. Donner, *J. Biol. Chem.*, 2007, **282**, 445–453.
7 G. Crevel, H. Bates, H. Huikeshoven and S. Cotterill, *J. Cell Sci.*, 2001, **114**, 2015–2025.

8 J. E. Bohonowych, U. Gopal and J. S. Isaacs, *J. Oncol.*, 2010, **2010**, 412985.
9 S. Takayama, J. C. Reed and S. Homma, *Oncogene*, 2003, **22**, 9041–9047.
10 L. Neckers, *J. Biosci.*, 2007, **32**, 517–530.
11 C. Jolly and R. I. Morimoto, *J. Natl. Cancer Inst.*, 2000, **92**, 1564–1572.
12 T. U. Mayer, T. M. Kapoor, S. J. Haggarty, R. W. King, S. L. Schreiber and T. J. Mitchison, *Science*, 1999, **286**, 971–974.
13 M. Maruya, M. Sameshima, T. Nemoto and I. Yahara, *J. Mol. Biol.*, 1999, **285**, 903–907.
14 T. Nemoto, Y. Ohara-Nemoto, M. Ota, T. Takagi and K. Yokoyama, *Eur. J. Biochem.*, 1995, **233**, 1–8.
15 F. Koga, K. Kihara and L. Neckers, *Anticancer Res.*, 2009, **29**, 797–807.
16 M. V. Powers, K. Jones, C. Barillari, I. Westwood, R. L. M. v. Montfort and P. Workman, *Cell Cycle*, 2010, **9**, 1542–1550.
17 J. D. Eskew, T. Sadikot, P. Morales, A. Duren, I. Dunwiddie, M. Swink, X. Zhang, S. Hembruff, A. Donnelly, R. A. Rajewski, B. S. Blagg, J. R. Manjarrez, R. L. Matts, J. M. Holzbeierlein and G. A. Vielhauer, *BMC Cancer*, 2011, **11**, 468.
18 R. C. Vasko, R. A. Rodriguez, C. N. Cunningham, V. C. Ardi, D. A. Agard and S. R. McAlpine, *ACS Med. Chem. Lett.*, 2010, **1**, 4–8.
19 V. C. Ardi, L. D. Alexander, V. A. Johnson and S. R. McAlpine, *ACS Chem. Biol.*, 2011, **6**, 1357–1366.
20 J. M. McConnell, L. D. Alexander and S. R. McAlpine, *Bioorg. Med. Chem. Lett.*, DOI: 10.1016/j.bmcl.2013.11.059.
21 C. L. Carroll, J. V. C. Johnston, A. Kekec, J. D. Brown, E. Parry, J. Cajica, I. Medina, K. M. Cook, R. Corral, P.-S. Pan and S. R. McAlpine, *Org. Lett.*, 2005, **7**, 3481–3484.
22 T. J. Styers, R. A. Rodriguez, P.-S. Pan and S. R. McAlpine, *Tetrahedron Lett.*, 2006, **47**, 515–517.
23 K. Otrubova, K. L. McGuire and S. R. McAlpine, *J. Med. Chem.*, 2007, **50**, 1999–2002.
24 P. S. Pan, K. McGuire and S. R. McAlpine, *Bioorg. Med. Chem. Lett.*, 2007, **17**, 5072–5077.
25 R. A. Rodriguez, P.-S. Pan, C.-M. Pan, S. Ravula, S. A. Lapera, E. K. Singh, T. J. Styers, J. D. Brown, J. Cajica, E. Parry, K. Otrubova and S. R. McAlpine, *J. Org. Chem.*, 2007, **72**, 1980–2002.
26 K. Otrubova, G. H. Lushington, D. Vander Velde, K. L. McGuire and S. R. McAlpine, *J. Med. Chem.*, 2008, **51**, 530–544.
27 P. S. Pan, R. C. Vasko, S. A. Lapera, V. A. Johnson, R. P. Sellers, C.-C. Lin, C.-M. Pan, M. R. Davis, V. C. Ardi and S. R. McAlpine, *Bioorg. Med. Chem.*, 2009, **17**, 5806–5825.
28 R. P. Sellers, L. D. Alexander, V. A. Johnson, C.-C. Lin, J. Savage, R. Corral, J. Moss, T. S. Slugocki, E. K. Singh, M. R. Davis, S. Ravula, J. E. Spicer, J. L. Oelrich, A. Thornquist, C.-M. Pan and S. R. McAlpine, *Bioorg. Med. Chem.*, 2010, **18**, 6822–6856.
29 J. B. Kunicki, M. N. Petersen, L. D. Alexander, V. C. Ardi, J. R. McConnell and S. R. McAlpine, *Bioorg. Med. Chem. Lett.*, 2011, **21**, 4716–4719.
30 M. R. Davis, E. K. Singh, H. Wahyudi, L. D. Alexander, J. Kunicki, L. A. Nazarova, K. A. Fairweather, A. M. Giltrap, K. A. Jolliffe and S. R. McAlpine, *Tetrahedron*, 2012, **68**, 1029–1051.
31 L. D. Alexander, J. R. Partridge, D. A. Agard and S. R. McAlpine, *Bioorg. Med. Chem. Lett.*, 2011, **21**, 7068–7071.
32 D. M. Ramsey, J. R. McConnell, L. D. Alexander, K. W. Tanaka, C. M. Vera and S. R. Mcalpine, *Bioorg. Med. Chem. Lett.*, 2012, **22**, 3287–3290.
33 V. C. Ardi, L. D. Alexander, V. A. Johnson and S. R. McAlpine, *ACS Chem. Biol.*, 2011, **6**, 1357–1366.
34 L. D. Alexander, J. R. Partridge, D. A. Agard and S. R. McAlpine, *Bioorg. Med. Chem. Lett.*, 2011, **21**, 7068–7071.
35 S. T. Diver and S. L. Schreiber, *J. Am. Chem. Soc.*, 1997, **119**, 5106–5109.
36 J. D. Klemm, S. L. Schreiber and G. R. Crabtree, *Annu. Rev. Immunol.*, 1998, **16**, 569–592.
37 B. R. Kusuma, L. B. Peterson, H. Zhao, G. Vielhauer, J. Holzbeierlein and B. S. Blagg, *J. Med. Chem.*, 2011, **54**, 6234–6253.
38 M. L. Miller, E. E. Roller, R. Y. Zhao, B. A. Leece, O. Ab, E. Baloglu, V. S. Goldmacher and R. V. J. Chari, *J. Med. Chem.*, 2004, **47**, 4802–4805.
39 M. M. U. Ali, S. M. Roe, C. K. Vaughan, P. Meyer, B. Panaretou, P. W. Piper, C. Prodromou and L. H. Pearl, *Nature*, 2006, **440**, 1013–1017.
40 D. R. Southworth and D. A. Agard, *Mol. Cell*, 2011, **42**, 771–781.
41 S. K. Wandinger, K. Richter and J. Buchner, *J. Biol. Chem.*, 2008, **283**, 18473–18477.
42 C.-C. Lee, T.-W. Lin, T.-P. Ko and A. H.-J. Wang, *PLoS One*, 2011, **6**, e19961.
43 Z. L. Hildenbrand, S. K. Molugu, N. Herrera, C. Ramirez, C. Xiao and R. A. Bernal, *Oncotarget*, 2011, **2**, 43–58.